Sensors and Actuators B 246 (2017) 1025–1029

Contents lists available at ScienceDirect

Sensors and Actuators B: Chemical

journal homepage: www.elsevier.com/locate/snb

Sensitivity of metal oxide gas sensors to non-parabolic intergranular barriers

C. Buono, D.A. Mirabella, C.M. Aldao*

Institute of Materials Science and Technology (INTEMA), University of Mar del Plata and National Research Council (CONICET), Juan B. Justo 4302, B7608FDQ Mar del Plata, Argentina

ARTICLE INFO

Article history:
Received 9 November 2016
Received in revised form 8 February 2017
Accepted 23 February 2017
Available online 1 March 2017

Keywords:
Gas sensors
Conductivity
Potential barriers

ABSTRACT

We analyze the electrical conductivity of polycrystalline semiconductor solids due to the presence of Schottky-type potential barriers formed at intergrains. The density of charged dopants along the grains is usually considered constant leading to parabolic intergranular potential barriers. If temperature is high enough to allow sufficiently mobility to the dopants, their resulting equilibrium distribution is far from constant leading to potential barriers that show a strong non-parabolic character. Implications for the electrical conductivity and then on the sensitivity to barrier height and sample doping in metal oxide gas sensors are discussed.

1. Introduction

The development of devices capable of monitoring physico-chemical phenomena through an electrical signal (sensors) has been motivated for domestic and industrial applications like control of environmental pollutants and dangerous emissions. In gas sensors based on polycrystalline semiconductors, the signal detection comes from the change of material resistivity after gas exposure. In particular, Schottky-type intergranular barriers are widely used to describe semiconductor interfaces such as those found in polycrystalline materials. Electron states at intergrains are responsible for barrier formation and it would be the basic mechanism in gas sensors. Since only a small amount of species adsorbed at grain boundaries affect potential barriers that control the film conductivity, this type of sensors is especially sensitive and then attractive to industrial applications [1–5].

The electrical conductivity in a semiconductor bulk is mainly controlled by imperfections in the crystalline structure. In practical semiconductors used in electronics, impurities are intentionally incorporated through chemical additives. Impurity atoms can behave as donors if they easily contribute with electrons to the conduction band or acceptors if they easily contribute with holes to the valence band. On the other hand, in semiconducting oxides native point defects are the main doping source as they spontaneously form in very high densities [6–8].

Regularly, large grains in polycrystalline semiconductors, used in gas sensing, present a surface space charge layer and an unaffected bulk. For n-type materials, the amount of negative surface charge associated to adsorbed oxygen ions (surface acceptor levels) is responsible for a barrier formation [1–5]. It is generally accepted that the surface space charge layer is responsible for band bending and the formation of parabolic barriers when a constant density of donors along the depletion region is assumed. Native point defects coming from oxygen vacancies (OV) are the main donor contribution in many oxides. Electrostatic interactions between charged OV affect their equilibrium distribution close to interfaces, given rise to surface barriers that are not parabolic [9]. Thus, it is expected that the non-parabolic character of the barriers affect the electrical conductivity since it does not only depend on the barriers height but also on the shape of the barriers, as is the case for tunneling current that depends on both [10–14].

In this work, we aim to present the effects of the donor distribution on intergranular barriers and then on conductivity of polycrystalline semiconductors. In particular, we focus our attention to the study of the defect concentrations along the depletion region accounting for the electric potential and compositional induced stresses. Variations of the electric potential in terms of the defect concentrations can be described using the Poisson–Boltzmann equation. For the spatial variations of the stress components within the solid, an elastic model is employed which relates stress components to the distribution of defect species in the particle [15]. The model is then applied to determine the donor concentration and then the intergranular potentials to finally calculate the resulting conductance.

* Corresponding author.
E-mail address: cmaldao@fi.mdp.edu.ar (C.M. Aldao).

http://dx.doi.org/10.1016/j.snb.2017.02.146
0925-4005/

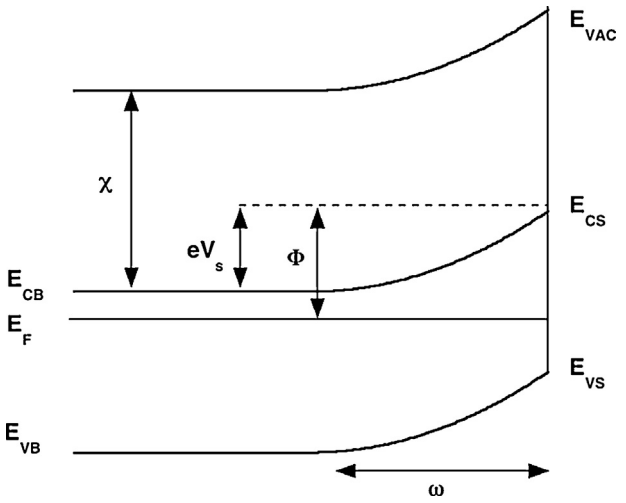

Fig. 1. Bands at a semiconductor surface illustrating the formation of the space charge region. ϕ is the work function, χ the electron affinity, eV_s the band bending, E_{VAC} the vacuum level, E_{CB} the bottom of the conduction band at the bulk, E_{CS} the bottom of the conduction band at the surface, E_{VB} the top of the valence band at the bulk, E_{VS} the top of the valence band at the surface, E_F the Fermi level, and ω the width of the depletion region.

2. Intergranular barriers

Fig. 1 shows an n-type semiconductor with surface states that can acquire a negative charge. The curvature of the bands is the band bending (denoted as eV_s) due to the positive charge at the depletion region (denoted as ω) and the negatively charged surface states.

In general, researchers in the field assume that the concentration of donors is uniform along the depletion region, which leads to Schottky-type intergranular barriers of parabolic shape [1]. However, in equilibrium, the donor density for singly ionized vacancies $N_d(x)$ is related to band bending as

$$N_d(x) = N_d \exp\left[\frac{(E_c(x) - E_{cb})}{kT}\right], \quad (1)$$

where N_d is the vacancy concentration in the bulk, T is the temperature, k is the Boltzmann constant, $E_c(x)$ is the bottom of the conduction band along the depletion region, and E_{cb} the bottom of the conduction band at the bulk, as shown in Fig. 1. The crucial point with Eq. (1) is that the equilibrium donor concentration strongly depends on band bending, as discussed in detail in Ref [16]. This issue, within the field of sensors, was raised by Lantto and co-workers long time ago [9]. He originally proposed that, if the temperature is high enough to allow sufficiently mobility to ionized oxygen vacancies, which play the role of donors in several oxides, they would tend to move toward the surface due to the present electric field, causing their rearrangement. Thus, the resulting distribution of donors in the depletion region is far from being constant. Eventually, there will be a concentration gradient responsible for a diffusion of vacancies in the opposite direction than that originated by the electric field. This analysis also leads to the distribution of Eq. (1).

Assuming that the only relevant charged particles are singly charged donors, by resorting to the Poisson's equation, the resulting potential $V(x)$ is given by

$$V(x) = \frac{kT}{2e} \log\left[1 + \tan^2\left(\frac{x}{\sqrt{2L_D}}\right)\right], \quad (2)$$

where $L_D = (\varepsilon kT/4e^2N_d)^{1/2}$ is the Debye length. This expression indicates that the potential grows very fast close to the surface.

Fig. 2(a) shows the concentration of donors in equilibrium $c(x)$ along the depletion layer for frozen donors (constant doping) and for single and doubly charged mobile donors, for a temperature $T = 600$ K, $\varepsilon = 10\varepsilon_0$, and a donor concentration in the bulk $N_d = 10^{23}$ m^{-3}. Interestingly, $c(x)$ along the depletion region dramatically changes when donors are mobile, from a constant distribution to a concentration gradient that becomes unphysically large near the surface.

Note that, the Coulomb interaction between the oxygen vacancies and negative charges at the interface produces a diffusion of vacancies to the intergrain surface and, for example, the concentration of donors vary from 10^{23} m^{-3} in the bulk to 10^{29} m^{-3} at the surface for doubly charged mobile donors (see Fig. 2(a)). Since charges correspond to oxygen vacancies, the above result implies doping concentration levels that lack of physical sense. This indicates that there must be a restriction in the concentration of donors. One possible restriction comes from the fact that the charge density

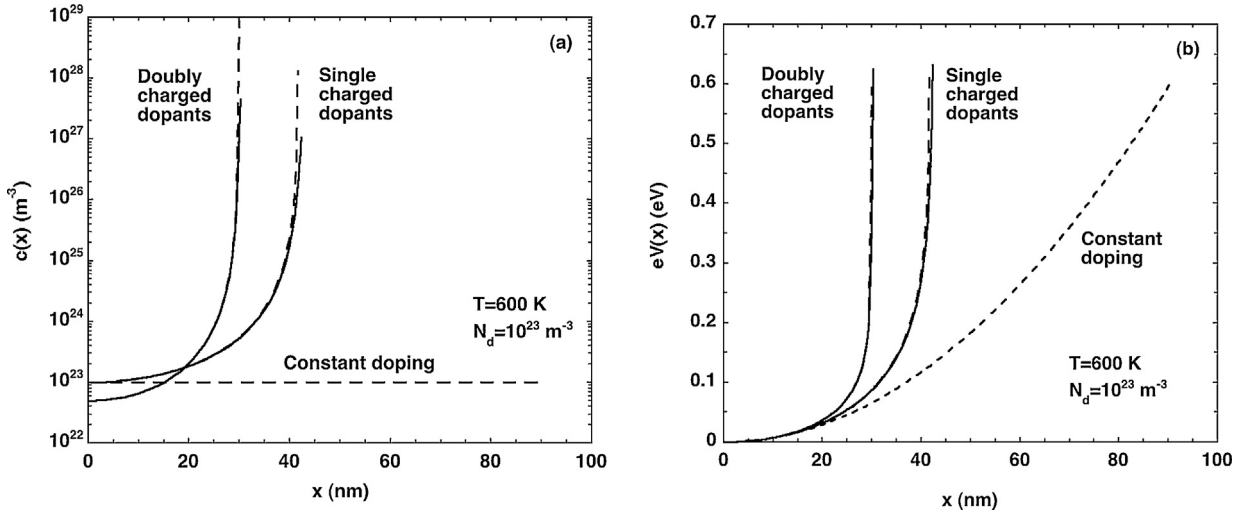

Fig. 2. (a) Dashed lines show the concentration for frozen donors (constant doping) and for singly and doubly charged mobile donors, at a temperature $T = 600$ K. In full lines, the concentrations of donors in equilibrium along the depletion region for mobile donors taking into account the elastic interaction given by Eq. (3). To have the same charge density at the bulk, for doubly charged donors, the donor concentration in the bulk was taken as a half of that corresponding to singly charged donors. (b) Electric potential for the concentrations given in (a). In the case of constant doping, $V(x)$ shows a parabolic shape. For singly and doubly mobile donors, $V(x)$ presents the Gouy–Chapman potential shape (dashed lines). The inclusion of the elastic contribution of Eq. (3) does no affect considerably the potential shape (full lines).

at the surface is constrained by the number of available sites. This is known as the Weisz limitation, which establishes a maximum value of density of charge in the surface of about 10^{17} m^{-2} [17].

If only electrostatic interaction between donors is taken into account the Weisz limitation is exceeded and the density of donors near the surface would adopt unphysical levels, as shown for mobile donors in Fig. 2(a); therefore, another interaction between donors must be operative. Indeed, vacancies repel each other not only due to the Coulomb interaction but also because of an elastic interaction. The elastic contribution is regularly much smaller than the Coulomb repulsion at not very far distances, but it becomes relevant for very high densities when the associated expansion or contraction of the crystal can induce a significant stress in the space charge region. The study of the consequences of this type of interaction through a mean field approach was the goal of a recent work [15]. In that paper, the authors proposed a new term proportional to the defect density, accounting for the elastic energy, which is added to the Coulomb interaction. Following Ref. [15], the elastic contribution E_s can be expressed as

$$E_s(x) = \beta\,[c(x) - c_0]\,, \tag{3}$$

with

$$\beta = \frac{4MV_0^2}{9V_m}, \tag{4}$$

where V_m is the molar volume, V_0 the partial molar volume of oxygen, and M the biaxial modulus. For tin oxide we can figure out $\beta = 2.46 \times 10^{-28}$ eV m^3.

Fig. 2(a) shows, in full lines, $c(x)$ in equilibrium along the depletion region for mobile donors taking into account the elastic interaction between them. The shape of $c(x)$ is very similar to that in which only the Coulomb interaction is taken into account, but the elastic interaction prevents that the concentration near the surface reaches unphysical values. In the case of constant doping, we present just one line because we are dealing with a jellium of non-interacting charge.

The vacancy concentration directly reflects on the shape of the electric potential and the band bending at the intergrain surface, which is commonly assumed as parabolic for a constant vacancy distribution. In Fig. 2(b) we plot the electric potential for the concentrations of Fig. 2(a). In the case of constant doping, $V(x)$ has the expected parabolic shape. For single- and double-ionized mobile donors, without the elastic interaction, $V(x)$ has the so-called Gouy–Chapman potential shape where the potential explodes near the surface. Interestingly, the inclusion of the elastic contribution of Eq. (3) does no affect considerably the potential shape.

3. Sensitivity

As described above, the mobility of donors, like oxygen vacancies in oxide semiconductors, dramatically affect potential barriers at the intergrains. We will illustrate that this has a strong effect on the conduction properties and then on the sensitivity to barrier changes of sensors based on this type of materials.

Main transport mechanisms that determine the conduction of Schottky barriers are emission of electrons over the top of the barrier, thermionic emission, and quantum-mechanical tunneling through the barrier. Regularly, researchers in the field of sensors only consider the thermionic-emission contribution. For a one-dimensional model representing the interface between two grains, the equilibrium thermionic current density is given by

$$J_{thermoionic} = AT^2 e^{-\phi/kT}, \tag{5}$$

where T is the absolute temperature, k is the Boltzmann constant, A is the Richardson constant, and ϕ is the barrier height.

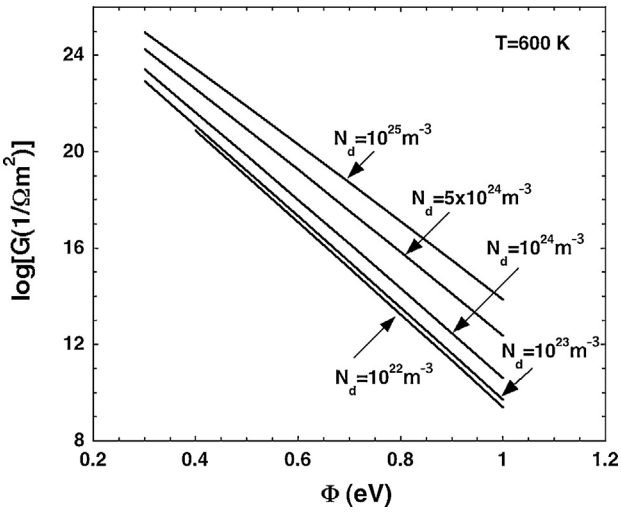

Fig. 3. Conductance per unit area as a function of barrier height for a parabolic potential for different doping concentration.

Additionally, electrons with energies below the top of the barrier can overcome the barrier by tunneling. This mechanism becomes dominant at low temperatures and high dopings [18]. For heavily doped semiconductors and low temperatures, tunneling mostly occurs for electrons with energies close to the Fermi level; this is known as field emission. At higher temperatures or lower doping, the maximum contribution occurs at energies above the bottom of the conduction band; this is known as thermionic-field emission. In equilibrium, the tunneling contribution can be calculated as [19]

$$J_{tunneling} = \frac{AT}{k}\int_0^{eV_s} F(E)\cdot P(E)dE, \tag{6}$$

where $F(E)$ is the Fermi–Dirac distribution function and $P(E)$ the transmission probability at energy E. Note that the first contribution given by Eq. (5) only depends on the barrier height and the contribution given by Eq. (6) depends on barrier height and width since $P(E)$ depends on the barrier shape. $P(E)$ can be calculated using the Wentzel–Kramers–Brillouin approximation as

$$P(E) = \exp\left[-2\int_a^b \alpha(x)dx\right] \tag{7}$$

where a and b correspond to the values of x where $E = V$ and α is given by

$$\alpha = 2\pi\frac{\sqrt{2m(V(x)-E)}}{h} \tag{8}$$

A double Schottky barrier model is widely accepted to describe polycrystalline semiconductor intergrains. However, many researchers consider grain boundaries of essentially zero width, while others take into account a non-negligible disordered layer at the grain boundaries, such that the electron transport occurs in two steps [10]. Since the main conclusions will not differ, for the sake of simplicity we adopted here the second assumption. Note that we are modeling a single barrier, which is directly connected to the polycrystal conductivity. This is correct as long as the polycrystal have large enough grains presenting a surface space charge layer and an unaffected bulk [20]. Also, we will assume that barriers are spatially uniform to allow a one-dimensional treatment [21].

Fig. 3 shows the conductance as a function of barrier height for a parabolic potential for different doping concentration in the bulk. In all our calculations, we adopted typical values for the effective mass ($m = 0.3m_e$) and for the relative permittivity ($\varepsilon = 10\varepsilon_0$). The

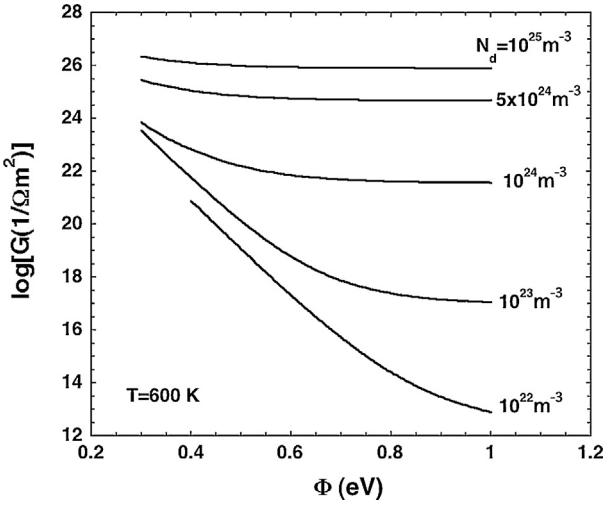

Fig. 4. Conductance per unit area as a function of the barrier height for Gouy–Chapman potential barriers for different donor concentration in the bulk.

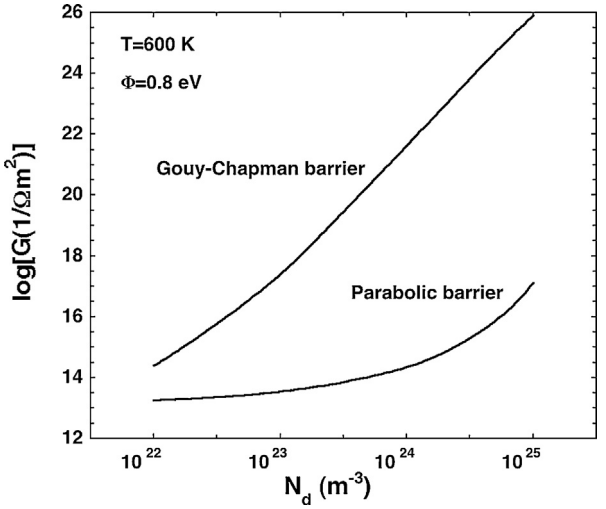

Fig. 5. Conductance per unit area as a function of the donor concentration in the bulk for a barrier height of 0.8 eV for the Gouy–Chapman potential and for the parabolic potential.

conductance decreases with the barrier height and increases with the donor concentration. As expected, the barrier height reduces the total conductance as directly affects the thermionic contribution. Also, the tunneling contribution is reduced, as a taller and wider barrier must be overcome. For a given barrier height, the conductance increases with doping because tunneling is favored as barriers become narrow.

Fig. 4 shows the conductance as a function of the barrier height for Gouy–Chapman potential barriers for different donor concentration in the bulk. Interestingly, for a sufficiently high donor concentration the conductance becomes independent of the barrier height in contrast to what one could expect. This effect is due to the fact that the electrical conductance is now dominated by tunneling current that is not affected by doping because of the strong non-parabolic character of the barrier.

Fig. 5 shows the electrical conductance as a function of the donor concentration in the bulk (barrier height of 0.8 eV and $T = 600$ K) for the Gouy–Chapman potential and for the parabolic potential. The conductance increases almost linearly with the logarithm of doping concentration for the Gouy–Chapman barrier in the range of the studied donor concentrations. The slope of the curve gives a

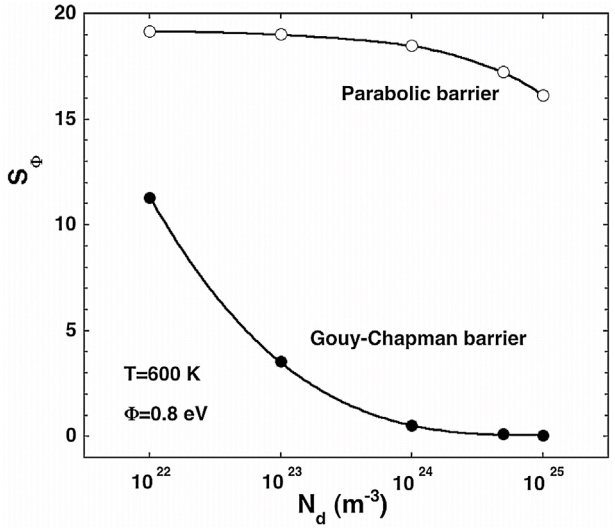

Fig. 6. Sensitivity to the barrier height for a parabolic and a Gouy–Chapman barriers.

measurement of the sensitivity of the material with the bulk doping. In short, following Figs. 4 and 5, the sensitivity with the doping concentration is higher than for parabolic barriers in most of the studied range, whereas for high vacancy concentrations it becomes independent of the barrier height.

In order to quantify the above statements, in Fig. 6 we present the conductance sensitivity to barrier height as a function of the bulk doping for a parabolic and a Gouy–Chapman barriers. We can define the sensitivity to the barrier height as

$$S_\Phi = \left| \frac{1}{G} \frac{\partial G}{\partial \Phi} \right| = \left| \frac{\partial \ln G}{\partial \Phi} \right|. \quad (9)$$

S_Φ can be determined from the results of Figs. 3 and 4 as the derivative of the curves for a specific barrier height. We chose $\Phi = 0.8$ eV as a typical barrier height value. For the parabolic barrier, as observed in Fig. 3, the slope reduces only slowly with the doping. Conversely, as it can also be seen in Fig. 4, the slope for the Gouy–Chapman barrier reduces abruptly with doping. For high doping, the Gouy–Chapman barrier becomes very narrow close to the surface and then an increase in its height does not affect the conductance because electrons can tunnel easily through the added portion to the original barrier.

Finally, in Fig. 7 we present the sensitivity to the bulk doping. In this case, we define the sensitivity as

$$S_N = \left| \frac{N_d}{G} \frac{\partial G}{\partial N_d} \right| = \left| N_d \frac{\partial \ln G}{\partial N_d} \right|. \quad (10)$$

In this expression S_N is measured as the rate between the relative change in conductance and the relative change in doping. At low doping, S_N for parabolic barriers is small because tunneling practically has no contribution in conduction, and the thermionic current is not affected. Conversely, for the Gouy–Chapman barrier, S_N is always large because tunneling contribution is dominant in all the studied doping range.

4. Conclusions

In this work we focus our attention to the basic understanding of the intergranular barriers responsible for polycrystalline semiconducting films conductivity. In particular, we found that, allowing mobility to ionized oxygen vacancies, the resulting equilibrium distribution of dopants leads to potential barriers that show a strong

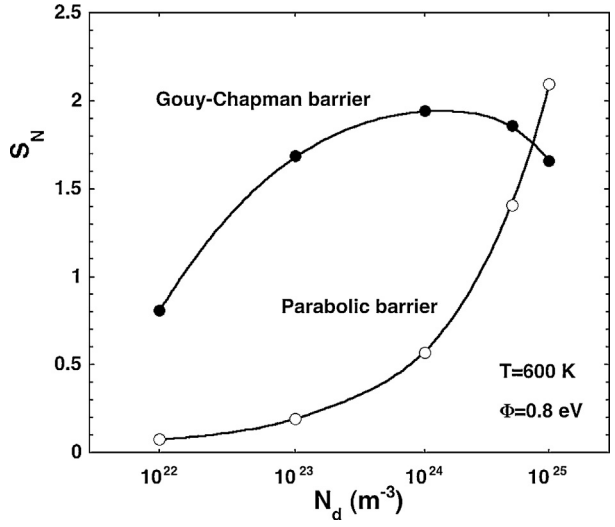

Fig. 7. Sensitivity to the bulk doping for a parabolic and a Gouy–Chapman barriers.

non-parabolic character, affecting the electrical conductivity and then the sensitivity of gas sensors.

When only Coulomb interactions between ionized oxygen vacancies are taken into account, the resulting donor concentration goes far beyond physical levels. This problem can be circumvented by including an elastic contribution that is not regularly considered. The resulting stress significantly alters defect concentrations naturally preventing the unphysical vacancy densities near the surface. Interestingly, we found that by including the elastic contribution, the potential shape at the depletion region is not seriously affected.

Then, we studied the changes of the conductance due to variations of the barrier height and doping. Results indicate that the effects on conductance of barrier height and doping strongly depend on the type of intergranular barriers we are assuming. Then, if potential barriers are non-parabolic, adopting a constant doping along the grains leads to wrong barrier characterization. This is crucial for researchers who attempt to study how adsorbed gases at the intergrains affect the intergranular barriers and then the resulting electrical properties. Also, we have shown that, at odds with parabolic barriers, changes in intergranular barrier heights can have small consequences while changes in doping can be responsible for large variations on conductance in a Gouy–Chapman barrier.

Acknowledgements

This work was partially supported by the National Council for Scientific and Technical Research (CONICET) of Argentina and the National University of Mar del Plata (Argentina).

References

[1] M.J. Madou, R. Morrison, Chemical Sensing with Solid State Devices, John Wiley & Sons, Inc., New York, 1989.
[2] N. Yamazoe, Toward innovations of gas sensor technology, Sens. Actuators B: Chem. 108 (2005) 2–14.
[3] N. Barsan, D. Koziej, U. Weimar, Metal oxide-based gas sensor research: how to? Sens. Actuators B: Chem. 121 (2007) 18–35.
[4] W. Gopel, K. Schierbaum, SnO_2 sensors: currents status and future prospect, Sens. Actuators B: Chem. 26 (1995) 1–12.
[5] N. Barsan, U. Weimar, Conduction model of metal oxide gas sensors, J. Electroceram. 7 (2001) 143–167.
[6] J. Maier, W. Gopel, Investigations of the bulk defect chemistry of polycrystalline tin(IV) oxide, J. Solid State Chem. 72 (1988) 293–302.
[7] S. Lany, A. Zunger, Dopability, intrinsic conductivity, and nonstoichiometry of transparent conducting oxides, Phys. Rev. Lett. 98 (2007) 045501.
[8] H.L. Tuller, S.R. Bishop, Point defects in oxides: tailoring materials through defect engineering, Annu. Rev. Mater. Res. 41 (2011) 369–398.
[9] P. Romppainen, V. Lantto, The effect of microstructure on the height of potential energy barriers in porous tin dioxide gas sensors, J. Appl. Phys. 63 (1988) 5159.
[10] M.S. Castro, C.M. Aldao, Prebreakdown conduction in zinc oxide varistors: thermionic or tunnel currents and one-step or two-step conduction processes, Appl. Phys. Lett. 63 (1993) 1077–1079.
[11] G. Blaustein, M.S. Castro, C.M. Aldao, Influence of frozen distributions of oxygen vacancies on tin oxide conductance, Sens. Actuators B 55 (1999) 33–37.
[12] M.A. Ponce, C. Malagù, M.C. Carotta, G. Martinelli, C.M. Aldao, Gas in-diffusion contribution to impedance in tin oxide thick films, J. Appl. Phys. 104 (2008) 054907.
[13] C.M. Aldao, F. Schipani, M.A. Ponce, E. Joanni, F.J. Williams, Conductivity in SnO_2 polycrystalline thick film gas sensors: tunneling electron transport and oxygen diffusion, Sens. Actuators B 193 (2014) 428–433.
[14] F. Schipani, D.R. Miller, M.A. Ponce, C.M. Aldao, S.A. Akbar, P.A. Morris, J.C. Xu, Conduction mechanisms in SnO_2 single-nanowire gas sensors: an impedance spectroscopy study, Sens. Actuators B 241 (2017) 99–108.
[15] B.W. Sheldon, V.B. Shenoy, Space charge induced surface stresses: implications in ceria and other ionic solids, Phys. Rev. Lett. 106 (2011) 216104.
[16] C.M. Aldao, C. Malagù, Non-parabolic intergranular barriers in tin oxide and gas sensing, J. Appl. Phys. 112 (2012) 024518.
[17] P.B. Weisz, Effects of electronic charge transfer between adsorbate and solid on chemisorption and catalysis, J. Chem. Phys. 21 (1953) 1531–1538.
[18] E.H. Rhoderick, R.H. Williams, Metal-Semiconductor Contacts, 2nd edn., Oxford Science, Cha, 1988, pp. 3.
[19] C.R. Crowell, V.L. Rideout, Normalized thermionic-field (T-F) emission in metal-semiconductor (Schottky) barriers, Solid-State Electron. 12 (1969) 89–105.
[20] G. Dezanneau, A. Morata, A. Tarancón, F. Peiró, J.R. Morante, Effect of grain size distribution on the grain boundary electrical response of 2D and 3D polycrystals, Solid State Ionics 177 (2006) 3117–3121.
[21] Y. Kajijawa, Conduction model covering non-degenerate through degenerate polycrystalline semiconductors with non-uniform grain-boundary potential heights based on an energy filtering model, J. Appl. Phys. 112 (2012) 123713.

Biographies

Camila Buono received her B.Sc. in 2010 and her Ph.D. in Physics in 2015 from the University of Mar del Plata, Argentina. She currently holds a post-doctoral position at the National Research Council (CONICET) in the Institute of Materials Science and Technology (INTEMA). Her main interests cover conduction mechanisms and sensing properties of gas sensors based on polycrystalline nanostructured semiconductors.

Daniel A. Mirabella received his B.Sc. in Computer Science in 1998 from CAECE University of Mar del Plata. His research activities focus on surface growth and physicochemistry of semiconductor surfaces and interfaces.

Celso M. Aldao completed his Ph.D. at the Department of Chemical Engineeringand Materials Science of the University of Minnesota in 1989. He was appointed as Professor in 1990 at the University of Mar del Plata. Since 1992 he is a member of the research staff of the National Research Council (CONICET). His research activities focus on the physics and chemistry of surfaces and interfaces, with special emphasison semiconductors.